JOURNAL OF GUIDANCE, CONTROL, AND DYNAMICS
Vol. 43, No. 9, September 2020

# Rigid-Body Pose Hybrid Control Using Dual Quaternions: Global Asymptotic Stabilization and Robustness

Bharani P. Malladi* and Eric A. Butcher†
*University of Arizona, Tucson, Arizona 85721*
and
Ricardo G. Sanfelice‡
*University of California, Santa Cruz, Santa Cruz, California 95064*

https://doi.org/10.2514/1.G004621

**A hybrid feedback control scheme is proposed for stabilization of rigid-body dynamics (position, orientation, and velocities) using unit dual quaternions, in which the dual quaternions and velocities are used for feedback. Specifically, both set-point stabilization and tracking control are addressed in this work. It is well known that rigid-body attitude control is subject to topological constraints, which often result in discontinuous control to avoid the unwinding phenomenon. In contrast, the hybrid scheme allows the controlled system to be robust in the presence of uncertainties, which would otherwise cause chattering about the point of discontinuous control while also ensuring acceptable closed-loop response characteristics. The stability of the closed-loop system is guaranteed through a Lyapunov analysis and the use of an invariance principle for hybrid systems. Simulation results for a rigid-body model are presented to illustrate the performance of the proposed hybrid dual-quaternion feedback control schemes.**



## Nomenclature

| | | |
|---|---|---|
| $\mathbb{N}$ | = | natural numbers, including 0 and which are equal to $\{0, 1, \ldots\}$ |
| $\mathbb{R}$ | = | the set of real numbers |
| $\mathbb{R}^n$ | = | $n$-dimensional Euclidean space |
| $\mathbb{R}_{\geq 0}$ | = | nonnegative real numbers, which are equal to $[0, \infty)$ |
| $\mathbb{Z}$ | = | integers |

## I. Introduction

RIGID-BODY control is often separated into two individual problems: attitude control (see [1–6]) and translational (point mass) control (see [7] and the references therein). However, for many practical applications that include robotics, computer graphics [8,9], unmanned air vehicle control, and spacecraft proximity operations [10–12] to name a few, these translational and rotational dynamics are often coupled. Hence, some recent research on controlling rigid-body dynamics uses the Lie group SE(3) for the configuration space (pose) of the rigid body and its tangent bundle TSE(3) for the state space, which includes velocities [13–15]. Tracking control of fully actuated vehicles is discussed in detail in [16]. Nevertheless, most of this work does not delve into the details of reconstructing the state of the system out of sensor measurements. To bypass this problem, a feedback law that directly uses vector measurements with the landmark-based control solution is presented in [17]. However, such strategies rely on continuous controllers, whereas it has been shown in [18] that global asymptotic stabilization of a given set point is not possible by means of continuous feedback. To solve this problem, continuous controllers based on the Morse–Lyapunov approach have been suggested in [2,19], which result in almost global asymptotic stability, whereas discontinuous control laws have been proposed (see, e.g., [20,21]) to achieve global asymptotic stability. However, the latter are not robust to small measurement noise, as shown by [22]. Recent advances in hybrid control theory have shown that well-posed hybrid systems, namely, those satisfying the so-called hybrid basic conditions [23], are inherently robust to small measurement noise, making hybrid control techniques suitable candidates for the problem at hand. In fact, hybrid control strategies using both quaternion feedback and rotation matrix feedback have been proposed in [22,24–29], respectively. Specifically on the tangent bundle TSE(3) associated with the special Euclidean group SE(3), Casau et al. [29] present an application of hybrid control strategies to underactuated vehicles, whereas Casau et al. [30] design hybrid control strategies for fully actuated rigid bodies with only landmark-based information.

Dual numbers introduced by Clifford [31] and later generalized by Study [32] are often used to parameterize SE(3). The advantage of using dual quaternions is that the rigid-body pose (position and orientation) can be represented in a compact form without separating the problem formulation into translational and rotational parts. It is a well-known fact that global asymptotic stabilization of rigid-body attitude is subject to topological constraints [33,34]. Hence, a rigid-body pose representation using unit dual quaternions (UDQs) inherits the same topological difficulties as the rigid-body attitude parameterization using unit quaternions (see [35,36] and the references therein). Specifically, a UDQ provides a dual cover for the elements in SE(3), that is, for every element in SE(3), there are exactly two UDQs. Because such a representation of rigid-body pose is nonunique, the control objective results in stabilizing a disconnected set of UDQs representing the same rigid-body position and orientation. Similar to the problem of rigid-body attitude stabilization in SO(3) [34], a continuous linear feedback law (as in [10,36,37]) results in the "unwinding" phenomenon, in which the feedback unnecessarily rotates the rigid body up to a full rotation. A discontinuous controller designed as in [38,39] would overcome such undesired large rotation, but is not robust to small measurement noise, and nonlinear controllers may suffer in terms of performance. Hybrid feedback control [23] can overcome such topological obstructions and provide robust global solutions for the rigid-body attitude stabilization problem [34]. In the case of full-state measurements (i.e., position, orientation, and linear and angular velocity measurements), Filipe and Tsiotras [10] present a continuous controller for rigid-body pose stabilization. Results associated with the kinematic subproblem of rigid-body motion using hybrid hysteresis-based UDQs are presented in [35], whereas an improved version using a bimodal approach to reduce higher average settling time or energy consumption is presented in [40]. In addition, model-predic-

Presented as Paper 2018-0606 at the AIAA Guidance, Navigation, and Control Conference, Kissimmee, FL, January 8–12, 2018; received 30 May 2019; revision received 30 January 2020; accepted for publication 4 February 2020; published online 6 July 2020. 

*Ph.D. Candidate, Department of Aerospace and Mechanical Engineering, 1130 N Mountain Avenue; malladi@email.arizona.edu. Student Member AIAA.

†Professor, Department of Aerospace and Mechanical Engineering, 1130 N Mountain Avenue; ebutcher@email.arizona.edu. Member AIAA.

‡Professor, Department of Electrical and Computer Engineering, 1156 High Street MS: SOE3; ricardo@ucsc.edu.

tive-control(MPC)-based dual-quaternion spacecraft pose control is presented in [41,42]. In this paper, we adapt the hysteresis-based switching strategy of rigid-body attitude presented in [33,34] to the UDQ parameterization of rigid-body pose. This paper combines the ideas of dual quaternions to represent rigid-body pose along with hybrid system theory to design feedback controllers for set-point stabilization and time-varying trajectory tracking problems. The proposed hybrid control strategies address shortcomings in some of the controllers previously proposed in the literature. Specifically, a complete solution for rigid-body kinematic and kinetic control is presented using a hybrid hysteresis-based switching strategy. Considering that the full-state (i.e., position, orientation, and linear and angular velocities) measurements are available for feedback, the following problems of interest are formalized in this paper:

1) A general hybrid feedback control solution with dual-quaternion and dual-velocity feedback for a rigid-body constant set-point pose stabilization is presented and its details are discussed in Sec. IV.A. Unlike [35], in which only the attitude and translational kinematics were treated, this paper treats hybrid control of both kinematics and kinetics.

2) The problem of tracking a time-varying reference is discussed in detail in Sec. IV.B. A hybrid control strategy to address a rigid-body pose tracking a time-varying reference is formulated. As an improvement to the results presented in [10,38,39], this paper establishes the robust global asymptotic stability of rigid-body set-point stabilization and time-varying reference tracking problems, respectively.

3) Robustness of the proposed algorithms to uncertainties is discussed in Sec. IV.C.

4) Numerical examples for a rigid-body set-point stabilization and time-varying reference tracking are given in Sec. V.

## II. Preliminaries

### A. Notation

The following notation and definitions are used throughout the paper. Given a vector $x \in \mathbb{R}^n$, $|x|$ denotes the Euclidean vector norm. $\mathbb{B}$ denotes the closed unit ball, of appropriate dimension, in a Euclidean norm. Given a set $S$, $\overline{S}$ denotes its closure. Given a point $x \in \mathbb{R}^n$, $|x|_S := \inf_{y \in S}|x - y|$. The equivalent notation $[x^\top \quad y^\top]^\top$, and $(x, y)$ is used for vectors. Given a vector $x \in \mathbb{R}^n$, $\nu(x) := [0 \quad x^\top]^\top$. Given a set $S$, $\overline{S}$ denotes its closure. Given a point $x \in \mathbb{R}^n$, $|x|_S := \inf_{y \in S}|x - y|$. An $n \times p$ zero vector/matrix is represented by $0_{n\times p}$. The unit quaternion with scalar part equal to one and the zero quaternion are given by $\mathbf{1} = (1, 0_{3\times1})$ and $\mathbf{0} = (0, 0_{3\times1})$, respectively. A function $\alpha: \mathbb{R}^+ \to \mathbb{R}_{\geq 0}$ is said to belong to class-$\mathcal{K}$ if it is continuous, zero at zero, and strictly increasing. A function $\alpha: \mathbb{R}^+ \to \mathbb{R}_{\geq 0}$ is said to belong to class-$\mathcal{K}_\infty$ if it belongs to class-$\mathcal{K}$ and is unbounded. A function $\beta: \mathbb{R}^+ \times \mathbb{R}^+ \to \mathbb{R}^+$ is said to belong to class-$\mathcal{KL}$ if it is nondecreasing in its first argument, nonincreasing in its second argument, and $\lim_{s \searrow 0}\beta(s, t) = \lim_{t\to\infty}\beta(s, t) = 0$.

### B. Well-Posed Hybrid Systems

Hybrid systems are dynamic systems with both continuous and discrete dynamics, in which a hybrid system $\mathcal{H} = (C, f, D, g)$ is defined by the following objects: 1) a mapping $f: \mathbb{R}^n \to \mathbb{R}^n$ called the *flow map*, 2) a mapping $g: \mathbb{R}^n \to \mathbb{R}^n$ called the *jump map*, 3) a set $C \subset \mathbb{R}^n$ called the *flow set*, and 4) a set $D \subset \mathbb{R}^n$ called the *jump set*. The flow map $f$ defines the continuous dynamics on the flow set $C$, whereas the jump map $g$ defines the discrete dynamics on the jump set $D$. These objects are referred to as the data of the hybrid system $\mathcal{H}$. Given a state $\chi$ of the hybrid system $\mathcal{H}$, the notation $\chi^+$ indicates the values of the state after the jump. A solution $\phi$ to $\mathcal{H}$ is given on extended time domain, called *hybrid time domain*, which is parameterized by the pairs $(t, j)$, where $t$ is the ordinary time component and $j$ is a discrete parameter that keeps track of the number of jumps; see [23]. Given a solution $\phi$ to $\mathcal{H}$, the notation $\mathrm{dom}\phi$ represents its domain, which is a hybrid time domain. A solution to $\mathcal{H}$ is said to be nontrivial if $\mathrm{dom}\phi$ contains at least one point different from $(0, 0)$; complete if $\mathrm{dom}\phi$ is unbounded; and maximal if it cannot be extended, that is, it is not a truncated version of another solution. The set $\mathcal{S}_{\mathcal{H}}(\xi)$ denotes the set of all maximal solutions to $\mathcal{H}$ from $\xi$.

### C. Rigid-Body Pose

The position and orientation of a rigid body with respect to a generic reference frame are defined by its relative position $p \in \mathbb{R}^3$ and its relative orientation $R \in \mathrm{SO}(3)$, which represents a rotation from the body frame to the inertial frame. Namely, its position $p$ and orientation $R$ form an element $(p, R)$ of the three-dimensional special Euclidean group $\mathrm{SE}(3) := \mathbb{R}^3 \times \mathrm{SO}(3)$. Given $(p, R) \in \mathrm{SE}(3)$, a UDQ associated with it is given by [43]

$$\hat{q} = q_r + \epsilon q_t \tag{1}$$

where

$$q_r = \begin{bmatrix} \eta_r \\ \mu_r \end{bmatrix} \in \mathcal{S}^3 : R = \mathcal{R}(q_r),$$

$$q_t = \begin{bmatrix} \eta_t \\ \mu_t \end{bmatrix} = \frac{1}{2}\nu(p) \otimes q_r \in \mathbb{H},$$

$\nu(p) = [0 \quad p^\top]^\top$, and $p \in \mathbb{R}^3$ is the position of the center of mass in inertial frame. Notice that the position of the rigid body in the body frame of reference is given by $\nu(p_b) = q_r^* \otimes \nu(p) \otimes q_r \in \mathbb{H}^v$, where $p_b \in \mathbb{R}^3$. A list of basic UDQ operations is given in the Appendix.

## III. Problem Description

Given an orthonormal inertial frame $\{I\}$ and an orthonormal body frame $\{B\}$, fixed to the rigid-body, its dynamic equations of motion in dual-quaternion representation [10,40] are given by (see Appendix for details)

$$\dot{\hat{q}}_b = \frac{1}{2}\hat{q}_b \otimes \nu(\hat{\omega}_b) \quad M \star \nu(\dot{\hat{\omega}}_b^s) = \hat{u} - \nu(\hat{\omega}_b) \times (M \star \nu(\hat{\omega}_b^s)) \tag{2}$$

where $\nu(\hat{\omega}_b) = (0 + \epsilon 0, \hat{\omega}_b) \in \hat{\mathbb{H}}^v$, $\nu(\hat{\omega}_b^s) = (0 + \epsilon 0, \hat{\omega}_b^s) \in \hat{\mathbb{H}}^v$, $\hat{\omega}_b^s = v_b + \epsilon\omega_b$, $\hat{\omega}_b = \omega_b + \epsilon v_b$, and $\omega_b, v_b \in \mathbb{R}^3$ are the linear and angular velocities of the rigid body with respect to the inertial frame $\{I\}$ represented in the body frame $\{B\}$, respectively; and $\hat{u} = \nu(F) + \epsilon\nu(\tau) \in \hat{\mathbb{H}}^v$, where $F \in \mathbb{R}^3$ represents control forces and $\tau \in \mathbb{R}^3$ represents control torques applied to the rigid body in its frame of reference. The dual inertia matrix (2) is given by

$$M = \begin{bmatrix} 1 & 0_{1\times3} & 0 & 0_{1\times3} \\ 0_{3\times1} & mI_3 & 0_{3\times1} & 0_{3\times3} \\ 0 & 0_{1\times3} & 1 & 0_{1\times3} \\ 0_{3\times1} & 0_{3\times3} & 0_{3\times1} & J \end{bmatrix} \tag{3}$$

where $m \in \mathbb{R}$ is the mass of the rigid body, $J = J^\top > 0$, and $J \in \mathbb{R}^{3\times3}$ is the mass moment of inertia of the body about its center of mass written in the body frame. Because the mass $m$ is positive and the inertia matrix $J$ is a real symmetric, positive-definite matrix, the dual inertia matrix $M$ in the aforementioned formulation is invertible.

With this dynamic model, the main goal of this paper was to design a controller that asymptotically stabilizes the rigid-body pose to a desired constant set point given by $(\hat{q}_d, \hat{\mathbf{0}}) \in \hat{\mathcal{S}}^3 \times \hat{\mathbb{H}}^v$ or time-varying reference position, orientation, and velocities, $t \mapsto (\hat{q}_d(t), \nu(\hat{\omega}_d(t))) \in \hat{\mathcal{S}}^3 \times \hat{\mathbb{H}}^v$, where $\hat{\omega}_d(t)$ is the dual velocity of the desired frame $\{D\}$ with respect to the inertial frame $\{I\}$ represented in the body frame $\{B\}$.

To formally present the problem, let us define the dual-quaternion and dual-velocity error variables of the body frame $\{B\}$ with respect to the desired frame $\{D\}$ resolved into $\{B\}$ as

$$\overline{q} := \hat{q}_d^* \otimes \hat{q}_b \in \hat{\mathcal{S}}^3, \qquad \nu(\overline{\omega}) := \nu(\hat{\omega}_b) - \nu(\hat{\omega}_d) \in \hat{\mathbb{H}}^v \tag{4}$$

Differentiating the aforementioned error variables and following [36,44] yield the error dynamics:

$$\dot{\overline{q}} = \frac{1}{2}\overline{q} \otimes \nu(\overline{\omega})$$
$$\nu(\dot{\overline{\omega}}^s) = M^{-1}\star(\hat{u} - \nu(\hat{\omega}_b) \times (M\star\nu(\hat{\omega}_b^s))) - \nu(\dot{\hat{\omega}}_d^s) \tag{5}$$

Then, in these error coordinates, convergence to the desired constant set point $(\hat{q}_d, \hat{\mathbf{0}})$ or to the time-varying reference $t \mapsto (\hat{q}_d(t), \nu(\hat{\omega}_d(t))) \in \hat{\mathcal{S}}^3 \times \hat{\mathbb{H}}^v$ reduces to $\overline{q}$ converging to the UDQ $\pm\hat{\mathbf{1}}$ and $\nu(\overline{\omega})$ converging to the dual quaternion $\hat{\mathbf{0}}$. With this reformulation, the problem we solve in this paper is stated as follows. For scenarios with full-state feedback, that is, the entire state $(\hat{q}_b, \hat{\omega}_b)$ is available for feedback:

*Problem 1:* Given a constant set-point reference pose $(\hat{q}_d, \hat{\mathbf{0}}) \in \hat{\mathcal{S}}^3 \times \hat{\mathbb{H}}^v$ or

*Problem 2:* Given a reference pose trajectory $t \mapsto (\hat{q}_d(t), \nu(\hat{\omega}_d(t))) \in \hat{\mathcal{S}}^3 \times \hat{\mathbb{H}}^v$

Design a control law assigning $\hat{u}$ in Eq. (2), such that the resulting closed-loop system satisfies the following properties:

1) Stability: trajectories to the closed-loop system in error coordinates $(\overline{q}, \nu(\overline{\omega}))$ are such that $\overline{q}$ stays close to either $\hat{\mathbf{1}}$ or $-\hat{\mathbf{1}}$, and $\nu(\overline{\omega})$ stays close to zero when they start close to each respective point.

2) Attractivity: in the error coordinates $(\overline{q}, \nu(\overline{\omega}))$, the $\overline{q}$ component converges to $\hat{\mathbf{1}}$ or $-\hat{\mathbf{1}}$, with zero linear and angular velocities $\nu(\overline{\omega})$.

3) Robustness: for each compact set of initial conditions and level of closeness to reference set point, there exists nonzero perturbation to the closed-loop system, such that, for each initial position, orientation, and linear and angular velocities of the rigid body in the said compact set, the resulting trajectories converge to nearby the set point, with a desired level of closeness.

## IV. Hybrid Feedback Control and Stability

Given the rigid-body kinematics and dynamics in error coordinates in Eq. (5), due to a desired constant or a time-varying structure of the reference given by $(\hat{q}_d, \hat{\mathbf{0}}) \in \hat{\mathcal{S}}^3 \times \hat{\mathbb{H}}^v$, $t \mapsto (\hat{q}_d(t), \nu(\hat{\omega}_d(t))) \in \hat{\mathcal{S}}^3 \times \hat{\mathbb{H}}^v$, respectively, in this section, we present the hybrid feedback control design for each of these cases separately.

### A. Problem 1: Rigid-Body Constant Set-Point Pose Stabilization

With the rigid-body kinematics and dynamics in error coordinates in Eq. (5), as in the scenario of Problem 1, consider that a constant set-point reference pose $(\hat{q}_d, \hat{\mathbf{0}}) \in \hat{\mathcal{S}}^3 \times \hat{\mathbb{H}}^v$ is given and the output of rigid-body dynamics [defined in Eq. (2)] $y = (\hat{q}_b, \hat{\omega}_b)$ is available for feedback. Hence, the error vector $(\overline{q}, \overline{\omega})$ defined in Eq. (4) is available for feedback. In addition, for the set-point stabilization problem, because the desired dual velocity $\nu(\hat{\omega}_d) = \hat{\mathbf{0}}$, the rigid-body kinematics and dynamics in error coordinates in Eq. (5) can be rewritten as follows:

$$\dot{\overline{q}} = \frac{1}{2}\overline{q} \otimes \nu(\overline{\omega}),$$
$$\nu(\dot{\overline{\omega}}^s) = M^{-1}\star(\hat{u} - \nu(\overline{\omega}) \times (M\star\nu(\overline{\omega}^s))) \tag{6}$$

A dual-quaternion-based control law for such a system in Eq. (6) is presented in [36] [theorem 1; Eq. (13)], which suffers from topological obstructions. To overcome this limitation and solve Problem 1, inspired by the formulation presented in [34], a dynamic feedback that depends on the logic variable $h \in \{-1, 1\} =: \mathcal{Q}$ is proposed. The proposed hybrid controller is given as follows:

$$\begin{aligned} \dot{h} &= 0 && (\overline{q}, \nu(\overline{\omega}), h) \in C, \\ h^+ &= -h && (\overline{q}, \nu(\overline{\omega}), h) \in D, \\ \hat{u} &= I_u\kappa(\overline{q}, \nu(\overline{\omega}), h) \end{aligned} \tag{7}$$

where

$$I_u := \begin{bmatrix} 0 & 0_{1\times 3} \\ 0_{3\times 1} & I_3 \end{bmatrix},$$
$$\kappa(\overline{q}, \nu(\overline{\omega}), h) := -hk_p(\overline{q}^* \otimes (h\overline{q}^s - \hat{\mathbf{1}}^s)) - k_d\nu(\overline{\omega}^s), \tag{8}$$

$k_p, k_d > 0$,

$$C = \{(\overline{q}, \nu(\overline{\omega}), h) \in \hat{\mathcal{S}}^3 \times \hat{\mathbb{H}}^v \times \mathcal{Q} : h\eta_r \geq -\delta\},$$
$$D = \{(\overline{q}, \nu(\overline{\omega}), h) \in \hat{\mathcal{S}}^3 \times \hat{\mathbb{H}}^v \times \mathcal{Q} : h\eta_r \leq -\delta\} \tag{9}$$

with $\delta \in (0, 1)$, and $\eta_r$ is the scalar part of rotational error quaternion $q_r \in \mathcal{S}^3$, where $\overline{q} = q_r + \epsilon q_t$. Hence, the hybrid closed-loop model of the rigid-body error kinematics and dynamics includes system (6) and the hybrid feedback controller (7–9). The closed-loop system denoted by $\mathcal{H} = (C, f, D, g)$ has state $\xi = (\overline{q}, \nu(\overline{\omega}), h) \in \hat{\mathcal{S}}^3 \times \hat{\mathbb{H}}^v \times \mathcal{Q} =: \mathcal{X}$ and hybrid dynamics

$$\dot{\xi} = f(\xi) \qquad \xi \in C, \quad \xi^+ = g(\xi) \qquad \xi \in D \tag{10}$$

Remark: As in previous work using models in terms of UDQs [10,36,37] and closed-loop systems with states using unit quaternions and logic variables [24,34], we treat the state space of the closed-loop system, namely, $\mathcal{X}$, as a set embedded in a large-enough Euclidean space [As in those references, this embedding allows us to employ notions for closedness of sets and continuity of maps that are standard in Euclidean spaces].

Details on hybrid system modeling are presented in Sec. II.B. The flow and jump sets satisfy $C \cup D = \mathcal{X}$, and the maps $f : \mathcal{X} \to \mathcal{X}$ and $g : \mathcal{X} \to \mathcal{X}$ are given by

$$f(\xi) := \begin{bmatrix} \frac{1}{2}\overline{q} \otimes \nu(\overline{\omega}) \\ M^{-1}\star(I_u\kappa(\xi) - \nu(\overline{\omega}) \times (M\star\nu(\overline{\omega}^s))) \\ 0 \end{bmatrix}, \quad g(\xi) := \begin{bmatrix} \overline{q} \\ \nu(\overline{\omega}^s) \\ -h \end{bmatrix} \tag{11}$$

Because of the design of the hybrid feedback (7–9), this hybrid system renders the compact set:

$$\mathcal{A} = \{\xi \in \mathcal{X} : \overline{q} = h\hat{\mathbf{1}}, \nu(\overline{\omega}^s) = \hat{\mathbf{0}}\} \tag{12}$$

globally asymptotically stable. (Details of this result are given in Theorem V.2.) Note that, for a constant set-point stabilization problem, the linear and angular velocities of the fixed frame $\nu(v_d) = \mathbf{0}$, $\nu(\omega_d) = \mathbf{0}$. Hence, in other words, set $\mathcal{A}$ represents the desired rigid-body pose error $\overline{q} = q_r + \epsilon q_t = h\hat{\mathbf{1}}$ and dual-velocity error $\nu(\overline{\omega}^s) = \nu(v_b - v_d) + \epsilon\nu(\omega_b - \omega_d) = \hat{\mathbf{0}}$ [i.e., the desired pose $q_r = \mathbf{1}$, $q_t = \mathbf{0}$, angular velocity $\nu(\omega_b) = \mathbf{0}$, and linear velocity $\nu(v_b) = \mathbf{0}$].

*Remark V.1:* Given the desired position, orientation, and velocities $(\hat{q}_d, \nu(\hat{\omega}_d)) \in \hat{\mathcal{S}}^3 \times \hat{\mathbb{H}}^v$, the first term in Eq. (8) can be written as

$$-hk_p(\overline{q}^* \otimes (h\overline{q}^s - \hat{\mathbf{1}}^s)) = -k_p(h\overline{q}^* \otimes (hq_t + \epsilon(hq_r - \mathbf{1}))) \tag{13}$$

Using the quaternion multiplication rule, Eq. (13) can be rewritten as follows:

$$-k_p h(\overline{q}^* \otimes (h\overline{q}^s - \hat{\mathbf{1}}^s)) = -k_p \begin{bmatrix} \eta_r\eta_t + \mu_r^\top\mu_t \\ \eta_r\mu_t - \eta_t\mu_r - \mu_r \times \mu_t \end{bmatrix} + \epsilon k_p \begin{bmatrix} 1 - h\eta_r + \eta_t^2 + \mu_t^\top\mu_t \\ -h\mu_r \end{bmatrix} \tag{14}$$

Therefore, the output of the dynamic feedback (7–9), using Eq. (4), can be rewritten as follows:

$$\hat{u} = \begin{bmatrix} 0 \\ -k_p(\eta_r\mu_t - \eta_t\mu_r) + k_p(\mu_r \times \mu_t) - k_d(v_b - v_d) \end{bmatrix} + \epsilon \begin{bmatrix} 0 \\ -hk_p\mu_r - k_d(\omega_b - \omega_d) \end{bmatrix} \tag{15}$$

Therefore, equating the input $\hat{u} = \nu(F) + \nu(\tau) \in \hat{\mathbb{H}}^v$ to Eq. (15) results in the following expression for the force $F \in \mathbb{R}^3$ and torque $\tau \in \mathbb{R}^3$:

$$\begin{aligned} F &= -k_p(\eta_r\mu_t - \eta_t\mu_r) + k_p(\mu_r \times \mu_t) - k_d(v_b - v_d), \\ \tau &= -hk_p\mu_r - k_d(\omega_b - \omega_d) \end{aligned} \tag{16}$$

Note that, for the set-point stabilization problem, namely, Problem 1, the linear and angular velocities $v_d$ and $\omega_d$ of the fixed desired frame satisfy $v_d = 0_{3\times1}$, $\omega_d = 0_{3\times1}$ in Eq. (16).

Next, the hybrid closed-loop system $\mathcal{H}$ satisfies the hybrid basic conditions (see [23], proposition 6.10), and our main result is as follows.

*Theorem V.2:* The set $\mathcal{A}$ in Eq. (12) is globally asymptotically stable for the closed-loop system $\mathcal{H}$.

*Proof:* For the hybrid closed-loop system (10), we first show that every complete solution to it converges to $\mathcal{A}$. For this purpose, we use the invariance principle for hybrid systems in [23] for which $\mathcal{H}$ has to satisfy the hybrid basic conditions, which is already the case from the hybrid system $\mathcal{H}$ formulation. After that, because $\mathcal{H}$ satisfies the hybrid basic conditions, following Proposition 6.10 in [23], we can conclude that every maximal solution to the hybrid system is complete, in this way showing the asymptotic stability of $\mathcal{A}$.

Now, to show convergence of complete solutions to $\mathcal{A}$, consider the Lyapunov function candidate $V: \mathcal{X} \to \mathbb{R}$ given by

$$V(\xi) = \mathbf{1}^\top \overline{V}(\xi) \quad \forall\, \xi \in \mathcal{X} \tag{17}$$

where $\overline{V}: \mathcal{X} \to \mathbb{H}^s$ is defined as

$$\overline{V}(\xi) := k_p(h\overline{q} - \hat{\mathbf{1}}) \circ (h\overline{q} - \hat{\mathbf{1}}) + \frac{1}{2}\nu(\overline{\omega}^s) \circ (M \star \nu(\overline{\omega}^s)) \quad \forall\, \xi \in \mathcal{X}$$

The constant $\hat{\mathbf{1}} = \mathbf{1} + \epsilon\mathbf{0}$, $\mathbf{1} = (1, 0_{3\times1})$, and $\circ$ operator for the UDQs is defined in item 8.d in the Appendix. With $q_r = (\eta_r, \mu_r) \in \mathcal{S}^3$, $q_t = (0, \mu_t) \in \mathbb{H}^v$ as defined in Eq. (1), $\nu(\omega) = (0, \omega_b) \in \mathbb{H}^v$, $\nu(v) = (0, v_b) \in \mathbb{H}^v$, as defined in Eq. (4), since $q_r \in \mathcal{S}^3$, $\eta_r^2 + \mu_r^\top\mu_r = 1$ and with $h^2 = 1$, Eq. (17) can be simplified as

$$V(\xi) = 2k_p(1 - h\eta_r) + k_p(\mu_t^\top\mu_t) + \frac{1}{2}(mv_b^\top v_b + \omega_b^\top J\omega_b) \tag{18}$$

The Lyapunov function in Eq. (18) satisfies $V(\xi) = 0$ for all $\xi \in \mathcal{A}$; $V(\xi) > 0$ for all $\xi \notin \mathcal{A}$. In addition, for any $c > 0$, there exists an $r > 0$, such that $V(\xi) > c$ whenever $|\xi| > r$. Thus, the set $\Omega_c := \{\xi \in \mathcal{X}: V(\xi) \le c\}$ is compact for every $c > 0$.

Next, the time derivative of the Lyapunov function candidate $V$ in Eq. (17) along the flows is given by

$$\begin{aligned} \frac{d}{dt}V(\xi) &= \mathbf{1}^\top\left(\frac{d}{dt}\overline{V}(\xi)\right) \\ &= \mathbf{1}^\top\Bigg(k_p h(h\overline{q} - \hat{\mathbf{1}}) \circ \frac{d}{dt}(\overline{q}) + k_p h\frac{d}{dt}(\overline{q}) \circ (h\overline{q} - \hat{\mathbf{1}}) \\ &\quad + \frac{1}{2}\nu(\overline{\omega}^s) \circ \left(M \star \frac{d}{dt}(\nu(\overline{\omega}^s))\right) + \frac{1}{2}\frac{d}{dt}(\nu(\overline{\omega}^s)) \circ (M \star \nu((\overline{\omega}^s)))\Bigg) \end{aligned} \tag{19}$$

[By $(d/dt)[V(\xi)]$, we mean the inner product between the gradient of $V$ and the vector field $f$ governing the continuous change of $\xi$ given in Eq. (10)].

Next, using the properties in items 10.c and 10.d of the Appendix, respectively

$$\frac{d}{dt}V(\xi) = \mathbf{1}^\top(2k_p h(h\overline{q} - \hat{\mathbf{1}}) \circ \frac{d}{dt}(\overline{q}) + \nu(\overline{\omega}^s) \circ \left(M \star \frac{d}{dt}(\nu(\overline{\omega}^s))\right)) \tag{20}$$

With $f$ in Eq. (10) and property 13 in the Appendix

$$\begin{aligned} \frac{d}{dt}V(\xi) &= \mathbf{1}^\top(2k_p h(h\overline{q} - \hat{\mathbf{1}}) \circ \left(\frac{1}{2}\overline{q} \otimes \nu(\overline{\omega})\right) \\ &\quad + \nu(\overline{\omega}^s) \circ M \star M^{-1}(I_u\kappa(\xi) - \nu(\hat{\omega}_b) \times (M \star \nu(\hat{\omega}_b^s)))) \end{aligned} \tag{21}$$

for each $\xi \in C$. Given $\overline{q}_1, \overline{q}_2, \overline{q}_3 \in \hat{\mathbb{H}}$, respectively, from the Appendix, following the property in item 10.a, the first term in Eq. (21) can be written as follows:

$$k_p h(h\overline{q} - \hat{\mathbf{1}}) \circ (\overline{q} \otimes \nu(\overline{\omega})) = \nu(\overline{\omega}^s) \circ (\overline{q}^* \otimes k_p h(h\overline{q}^s - \epsilon\mathbf{1})) \tag{22}$$

Next, the second term in Eq. (21) with $\hat{u} = I_u\kappa(\xi)$ is given by

$$\begin{aligned} &\nu(\overline{\omega}^s) \circ (\hat{u} - \nu(\overline{\omega}) \times (M \star \nu(\overline{\omega}^s))) \\ &= \nu(\overline{\omega}^s) \circ \hat{u} - \nu(\overline{\omega}^s) \circ (\nu(\overline{\omega}) \times (M \star \nu(\overline{\omega}^s))) \end{aligned} \tag{23}$$

Using the operation in items 10.b and 10.f along with the cross-product operation of the dual quaternion in item 10.g of the Appendix, the second term in Eq. (23) results in the following:

$$\nu(\overline{\omega}^s) \circ (\nu(\overline{\omega}) \times (M \star \nu(\overline{\omega}^s))) = \hat{\mathbf{0}}$$

Then, combining these steps, we have

$$\begin{aligned} &\nu(\overline{\omega}^s) \circ (\hat{u} - \nu(\overline{\omega}) \times (M \star \nu(\overline{\omega}^s))) \\ &= \nu(\overline{\omega}^s) \circ I_u\kappa(\xi) - \nu(\overline{\omega}^s) \circ (\nu(\overline{\omega}) \times (M \star \nu(\overline{\omega}^s))), \\ &= \nu(\overline{\omega}^s) \circ I_u\kappa(\xi) \end{aligned} \tag{24}$$

Therefore, from Eqs. (22) and (23), since $k_p > 0$ is a constant and $h \in \mathcal{Q}$

$$\begin{aligned} \frac{d}{dt}V(\xi) &= \mathbf{1}^\top(\nu(\overline{\omega}^s) \circ (\overline{q}^* \otimes k_p h(h\overline{q}^s - \epsilon\mathbf{1})) + \nu(\overline{\omega}^s) \circ I_u\kappa(\xi)), \\ &= \mathbf{1}^\top(\nu(\overline{\omega}^s) \circ (k_p h\overline{q}^* \otimes (h\overline{q}^s - \epsilon\mathbf{1}) + I_u\kappa(\xi))) \end{aligned}$$

From Eq. (8), since $I_u\kappa(\xi) = I_u(-k_p h\overline{q}^* \otimes (h\overline{q}^s - \hat{\mathbf{1}}^s) - k_d\nu(\overline{\omega}^s)) \in \hat{\mathbb{H}}$, we get

$$\begin{aligned} \frac{d}{dt}V(\xi) &= \mathbf{1}^\top(\nu(\overline{\omega}^s) \circ (k_p h\overline{q}^* \otimes (h\overline{q}^s - \epsilon\mathbf{1}) + I_u(-k_p h\overline{q}^* \otimes (h\overline{q}^s - \epsilon\mathbf{1})))) \\ &\quad - \mathbf{1}^\top(k_d\nu(\overline{\omega}^s) \circ \nu(\overline{\omega}^s)) \end{aligned} \tag{25}$$

where

$$I_u = \begin{bmatrix} 0 & 0_{1\times3} \\ 0_{3\times1} & I_3 \end{bmatrix}, \qquad k_p, k_d > 0$$

With the $\circ$ operator defined in item 8.d in the Appendix, the nonvelocity term in Eq. (25), using the definitions $v = v_b - v_d$, $\omega = \omega_b - \omega_d$ (for notational simplicity), reduces to

$$\frac{d}{dt}V(\xi) = -\mathbf{1}^\top(k_d\nu(\overline{\omega}^s) \circ \nu(\overline{\omega}^s)) = -k_d\omega^\top\omega - k_d v^\top v \tag{26}$$

Therefore, from Eq. (26), defining, for each $\xi \in C$

$$u_C(\xi) := \begin{cases} -k_d\omega^\top\omega - k_d v^\top v & \text{if } \xi \in C \\ -\infty & \text{otherwise} \end{cases} \tag{27}$$

we can see that $\frac{d}{dt}V(\xi) = u_C(\xi) \leq 0$.

Next, at jumps, for each $\xi \in D$, the Lyapunov function candidate $V$ in Eq. (17) changes as follows:

$$V(g(\xi)) - V(\xi) = \mathbf{1}^\top(k_p((-h\overline{q}-\hat{\mathbf{1}})\circ(-h\overline{q}-\hat{\mathbf{1}})) - ((h\overline{q}-\hat{\mathbf{1}})\circ(h\overline{q}-\hat{\mathbf{1}})))$$

Given $\overline{q} := q_r + \epsilon q_t$, where $q_r = (\eta_r, \mu_r) \in \mathcal{S}^3, q_t = (0, \mu_t) \in \mathbb{H}^v$ are defined in Eq. (1):

$$\begin{aligned} &V(g(\xi)) - V(\xi) \\ &= \mathbf{1}^\top(k_p((-h(q_r+\epsilon q_t)-\hat{\mathbf{1}})\circ(-h(q_r+\epsilon q_t)-\hat{\mathbf{1}})) \\ &\quad - ((h(q_r+\epsilon q_t)-\hat{\mathbf{1}})\circ(h(q_r+\epsilon q_t)-\hat{\mathbf{1}}))) \\ &= k_p(\mu_r\cdot\mu_r + (h\eta_r+1)^2 - \mu_r\cdot\mu_r - (h\eta_r-1)^2) = 4k_p h\eta_r \end{aligned} \tag{28}$$

Because, for each point $\xi$ in $D$, $h\eta_r \leq -\delta$

$$V(g(\xi)) - V(\xi) \leq -4k_p\delta$$

Defining, for each $\xi \in D$

$$u_D(\xi) := \begin{cases} -4k_p\delta & \text{if } \xi \in D \\ -\infty & \text{otherwise} \end{cases} \tag{29}$$

we have $V(g(\xi)) - V(\xi) = u_D(\xi) < 0$ for all $\xi \in D \setminus \mathcal{A}$.

*1. Completeness of Maximal Solutions*

We have that $u_C(\xi)$ and $u_D(\xi)$ are nonpositive for all $\xi \in \mathcal{X}$. And hence, every solution $\phi \in \mathcal{S}_{\mathcal{H}}(\phi(0,0))$, where $\phi(0,0) \in \mathcal{X}$ to the hybrid system in Eq. (10) remains in $\mathcal{X}$ for all $(t, j) \in \text{dom}(\phi)$. Also, $\mathcal{A}$ is compact and the Lyapunov function $V$ is positive definite relative to $\mathcal{A}$, the sublevel set $\Omega_c := \{\xi \in \mathcal{X}: V(\xi) \leq c\}$ is compact for every $c > 0$, and $V$ is nonincreasing along the solutions of $\mathcal{H}$. These results show that any solution $\phi$ to the hybrid system $\mathcal{H}$ is bounded and does not blow up in finite time. Also, $g(D) \subset C \cup D$, which shows that every solution $\phi$ to system $\mathcal{H}$ does not jump out of $C \cup D$. Therefore, from [23] (proposition 2.10), because conditions $(b)$ and $(c)$ therein are not satisfied, we conclude that every maximal solution to the closed-loop system $\mathcal{H}$ is complete.

*2. Application of Invariance Principle for Hybrid Systems*

The growth of $V$ along the solutions to $\mathcal{H}$ is bounded by $u_C(\xi)$ and $u_D(\xi)$ on $\mathcal{X}$. Because $\mathcal{H}$ satisfies the hybrid basic conditions and $V$ in Eq. (17) is continuous, the invariance principle for hybrid systems given in Theorem 8.2 of [23] implies that every precompact (complete and bounded) solution to the hybrid system (10) converges to the largest weakly invariant set $W$ contained in

$$V^{-1}(a) \cap \mathcal{X} \cap \left[\overline{u_C^{-1}(0)} \cup (u_D^{-1}(0) \cap g(u_D^{-1}(0)))\right] \tag{30}$$

for some $a \in \mathbb{R}_{\geq 0}$. Note that, for every point in $\hat{\mathcal{S}}^3, \overline{\mu} = \mu_r + \epsilon\mu_t = 0_{3\times1} + \epsilon 0_{3\times1}$ implies $\overline{\eta} = \eta_r + \epsilon\eta_t = \pm 1 + \epsilon 0$. By evaluating the dynamics (10) along solutions that remain in Eq. (30), we have that $\nu(\overline{\omega}) \equiv \hat{\mathbf{0}}$. Therefore, with $f$ in Eq. (10) and the expression of input $\hat{u}$ in Eq. (15), $\nu(\overline{\omega}^s) \equiv \hat{\mathbf{0}}$ implies $\overline{\mu} = \mu_r + \epsilon\mu_t = 0_{3\times1} + \epsilon 0_{3\times1}$, and since $h\eta_r \geq -\delta$ with $\delta \in (1, 0)$, then for all $\xi \in \mathcal{X} \cap \overline{u_C^{-1}(0)}$, $\overline{q} = h\hat{\mathbf{1}}$. Hence

$$\begin{aligned} W &\subset \{\xi \in \mathcal{X}: h\eta_r \geq -\delta, \eta_r = \pm 1, \mu_r = 0_{3\times1}, \eta_t = 0, \mu_t \\ &= 0_{3\times1}, \nu(\overline{\omega}^s) = \hat{\mathbf{0}}\} \cap V^{-1}(a) \\ &\subset \{\xi \in \mathcal{X}: \overline{q} = h\hat{\mathbf{1}}, \nu(\overline{\omega}^s) = \hat{\mathbf{0}}\} \cap V^{-1}(a) \end{aligned}$$

Then, because the only invariant set is for $a = 0$, Eq. (30) with $a = 0$ is contained in $\mathcal{A}$, that is

$$W \subset \{\xi \in \mathcal{X}: \overline{q} = h\hat{\mathbf{1}}, \nu(\overline{\omega}^s) = \hat{\mathbf{0}}\} \cap V^{-1}(0) \subset \mathcal{A}$$

Because every maximal solution to $\mathcal{H}$ is precompact, each maximal solution $\phi$ to $\mathcal{H}$ converges to $\mathcal{A}$. We conclude that $\mathcal{A}$ is globally attractive for the hybrid system $\mathcal{H}$. Because the function $V$ in Eq. (17) is positive definite relative to $\mathcal{A}$ and nonincreasing along the solutions of $\mathcal{H}$, $\mathcal{A}$ is stable for the closed-loop hybrid system. Hence, we conclude that the set $\mathcal{A}$ is globally asymptotically stable for the hybrid system $\mathcal{H}$. □

### B. Problem 2: Rigid-Body Time-Varying Reference Pose Tracking

Let us consider the rigid-body dynamics between an orthonormal inertial frame $\{I\}$ and an orthonormal body frame $\{B\}$, as outlined in Sec. III. Let $t \mapsto x_d(t) := (p_d, q_d, v_d, \omega_d)(t)$ denote a smooth trajectory evolving on $\mathcal{S}^3 \times \mathbb{R}^9$ for all $t \geq 0$ satisfying the following assumption:

*Assumption V.3:* Let $\pi: \mathcal{S}^3 \times \mathbb{R}^9 \to \mathcal{S}^3 \times \mathbb{R}^3$ denote the canonical projection of $\mathcal{S}^3 \times \mathbb{R}^9$ on to $\mathcal{S}^3 \times \mathbb{R}^3$. The reference trajectory $t \mapsto x_d(t) := (p_d, q_d, v_d, \omega_d)(t)$ is a complete and bounded solution to $\dot{x_d} = \zeta(x_d)$ satisfying

$$\begin{aligned} &\frac{d}{dt}\pi(p_d(t), q_d(t), v_d(t), \omega_d(t)) \\ &\quad = (v_d(t) - S(\omega_d(t))p_d(t), \frac{1}{2}q_d(t) \otimes \omega_d(t)) \end{aligned} \tag{31}$$

for each $t \geq 0$ and for some continuously differentiable vector field $\zeta$ on $\mathcal{S}^3 \times \mathbb{R}^9$.

To this trajectory $t \mapsto x_d(t)$ satisfying Assumption V.3, for each $t \geq 0$, one may associate a desired reference frame $\{D\}$. The origin of such a desired reference frame is located at $p_d(0) \in \mathbb{R}^3$ with orientation given by $q_d(0) \in \mathcal{S}^3$. In addition, a UDQ associated with this desired reference frame is given by [43]

$$t \mapsto \hat{q}_d(t) := q_d(t) + \epsilon q_{d_t}(t) \tag{32}$$

where $t \mapsto q_{d_t}(t) = (1/2)q_d(t) \otimes \nu(p_d(t)) \in \mathbb{H}^v$ for all $t \geq 0$. With this desired frame reference trajectory, the main goal in this section is as follows:

*Problem 2:* Given a reference trajectory $t \mapsto (\hat{q}_d(t), \hat{\omega}_d(t)) \in \hat{\mathcal{S}}^3 \times \hat{\mathbb{H}}^v$, design a control law as a function of the sensor outputs and the reference trajectory $t \mapsto (\hat{q}_d(t), \hat{\omega}_d(t)) \in \hat{\mathcal{S}}^3 \times \hat{\mathbb{H}}^v$, such that

$$\lim_{t\to\infty} \overline{q}(t) = \pm\hat{\mathbf{1}}, \qquad \lim_{t\to\infty} \overline{\omega}(t) = \hat{\mathbf{0}}$$

for all initial conditions, where

$$\overline{q} = \hat{q}_d^* \otimes \hat{q}_b \in \hat{\mathcal{S}}^3, \qquad \nu(\overline{\omega}) := \nu(\hat{\omega}_b) - \nu(\hat{\omega}_d) \in \hat{\mathbb{H}}^v \tag{33}$$

$(\hat{q}_b, \hat{\omega}_b) \in \hat{\mathcal{S}}^3 \times \hat{\mathbb{H}}^v$ is the state of the orthonormal body frame $\{B\}$, is outlined in Sec. IV. Differentiating the error variables in Eq. (33), following [36,44], the dynamics of the error variables are given as follows:

$$\begin{aligned} \dot{\overline{q}} &= \frac{1}{2}\overline{q} \otimes \nu(\overline{\omega}) \\ \dot{\nu(\overline{\omega}^s)} &= M^{-1}\star(\hat{u} - (\nu(\overline{\omega}) + \nu(\hat{\omega}_d)) \times (M\star(\nu(\overline{\omega}^s) + \nu(\hat{\omega}_d^s))) \\ &\quad - M\star\nu(\dot{\hat{\omega}}_d^s)) \end{aligned} \tag{34}$$

where $\hat{u} \in \hat{\mathbb{H}}^v$ is the total dual force resolved into the body frame. Therefore, to solve Problem 2, let us consider a hybrid feedback, similar to the hybrid controller in Eq. (7), which depends on the logic variable $h \in \{-1, 1\} =: \mathcal{Q}$, along with a feedforward term that

depends on a reference input $(\nu(\hat{\omega}_d^s), \nu(\dot{\hat{\omega}}_d^s)) \in \hat{\mathbb{H}}^v \times \hat{\mathbb{H}}^v$, given as follows. [We consider that the reference input is generated on the hybrid time domain $(t, j) \mapsto (\nu(\hat{\omega}_d^s(t, j)), \nu(\dot{\hat{\omega}}_d^s(t, j)))$.]

$$\begin{aligned} \dot{h} &= 0 && (\overline{q}, \nu(\overline{\omega}), h) \in C, \\ h^+ &= -h && (\overline{q}, \nu(\overline{\omega}), h) \in D, \\ \hat{u} &= I_u \tilde{\kappa}(\overline{q}, \nu(\overline{\omega}), h, \nu(\hat{\omega}_d^s), \nu(\dot{\hat{\omega}}_d^s)) \end{aligned} \tag{35}$$

where

$$I_u = \begin{bmatrix} 0 & 0_{1\times 3} \\ 0_{3\times 1} & I_3 \end{bmatrix},$$

$$\tilde{\kappa}(\overline{q},\nu(\overline{\omega}),h,\nu(\hat{\omega}_d^s),\nu(\dot{\hat{\omega}}_d^s)) := \kappa_{\text{fb}}(\overline{q},\nu(\overline{\omega}),h,\nu(\hat{\omega}_d^s)) + \kappa_{\text{ff}}(\nu(\hat{\omega}_d^s),\nu(\dot{\hat{\omega}}_d^s)) \tag{36}$$

the terms

$$\begin{aligned} \kappa_{\text{fb}}(\overline{q}, \nu(\overline{\omega}), h, \nu(\hat{\omega}_d^s)) &= \kappa(\overline{q}, \nu(\overline{\omega}), h) + \nu(\overline{\omega}) \times (M \star \nu(\hat{\omega}_d^s)) \\ &\quad + \nu(\hat{\omega}_d) \times (M \star \nu(\overline{\omega}^s)), \\ \kappa_{\text{ff}}(\nu(\hat{\omega}_d^s), \nu(\dot{\hat{\omega}}_d^s)) &= \nu(\hat{\omega}_d) \times (M \star \nu(\hat{\omega}_d^s)) + M \star \nu(\dot{\hat{\omega}}_d^s) \end{aligned}$$

The constants $k_p, k_d > 0$, and the function $\kappa(\overline{q}, \nu(\overline{\omega}), h)$ is given in Eq. (8)

$$\begin{aligned} C &= \{(\overline{q}, \nu(\overline{\omega}), h) \in \hat{\mathcal{S}}^3 \times \hat{\mathbb{H}}^v \times \mathcal{Q} : h\eta_r \geq -\delta\}, \\ D &= \{(\overline{q}, \nu(\overline{\omega}), h) \in \hat{\mathcal{S}}^3 \times \hat{\mathbb{H}}^v \times \mathcal{Q} : h\eta_r \leq -\delta\} \end{aligned} \tag{37}$$

with $\delta \in (0, 1)$, and $\eta_r$ is the scalar part of rotational error quaternion $q_r \in \mathcal{S}^3$.

The hybrid closed-loop model for the rigid-body tracking error kinematics and dynamics includes system (34) and the hybrid controller given in Eqs. (35–37). The closed-loop system denoted by $\mathcal{H}_T = (C, f, D, g)$ has state $\xi = (\overline{q}, \nu(\overline{\omega}), h) \in \hat{\mathcal{S}}^3 \times \hat{\mathbb{H}}^v \times \mathcal{Q} =: \mathcal{X}$ and hybrid dynamics represented by Eq. (10). The flow and jump sets satisfy $C \cup D = \mathcal{X}$, and due to the design of the controller (35–37), the maps $f : \mathcal{X} \to \mathcal{X}$ and $g : \mathcal{X} \to \mathcal{X}$ are given by

$$f(\xi) := \begin{bmatrix} \frac{1}{2}\overline{q} \otimes \nu(\overline{\omega}) \\ M^{-1} \star (I_u \kappa(\xi) - \nu(\overline{\omega}) \times (M \star \nu(\overline{\omega}^s))) \\ 0 \end{bmatrix}, \quad g(\xi) := \begin{bmatrix} \overline{q} \\ \nu(\overline{\omega}^s) \\ -h \end{bmatrix} \tag{38}$$

Therefore, the objective specified in Problem 2 is equivalent to the global asymptotic stabilization of set $\mathcal{A}$ in Eq. (12). Next, this hybrid closed-loop system $\mathcal{H}_T$ satisfies the hybrid basic conditions (see [23], proposition 6.10). The next result states that the proposed hybrid controller solves the rigid-body pose tracking problem in Problem 2.

*Theorem V.4:* Set $\mathcal{A}$ in Eq. (12) is globally asymptotically stable for the closed-loop system $\mathcal{H}_T$.

*Proof:* With the choice of the hybrid feedback and the feedforward terms in Eq. (36), the hybrid closed-loop model for the time-varying reference pose tracking (38) reduces to the hybrid model for constant set-point pose stabilization (11). Because the dynamics of the hybrid closed-loop system $\mathcal{H}_T$ in Eq. (38) match the dynamics of the hybrid system $\mathcal{H}$ in Eq. (11), the proof of this theorem follows the proof of Theorem V.2. □

### C. Robustness of the Closed-Loop System

To be able to cope with perturbations arising in real-world settings, let us consider that the plant (10) or (38) is affected by unmodeled dynamics given by $\hat{e} = (e_1, 0) + \epsilon(e_2, 0) \in \mathcal{X}$, $e_i \in \mathbb{R}^8$, $i \in \{1, 2\}$, and measurement error $\hat{m} = (m_1, 0) + \epsilon(m_2, 0) \in \mathcal{X}$, $m_i \in \mathbb{R}^8$, $i \in \{1, 2\}$, respectively, resulting in a perturbed closed-loop system with continuous dynamics and measurements:

$$\dot{\xi} = f(\xi) + \hat{e} \quad y = (\overline{q}, \overline{\omega}) + \hat{m} \tag{39}$$

where the error parameters in the original coordinates $\xi = (\overline{q}, \nu(\overline{\omega}), h) \in \hat{\mathcal{S}}^3 \times \hat{\mathbb{H}}^v \times \mathcal{Q} =: \mathcal{X}$ can also be defined as $\hat{e} = (\hat{e}_q, \hat{e}_\omega, 0) \in \mathcal{X}$, $\hat{e}_q := (e_{1_r} + \epsilon e_{2_r}) \in \hat{\mathcal{S}}^3$, $\hat{e}_\omega := (e_{1_\omega} + \epsilon e_{2_v}) \in \hat{\mathbb{H}}^v$, $\hat{m} = (\hat{m}_q, \hat{m}_\omega, 0) \in \mathcal{X}$, $\hat{m}_q := (m_{1_r} + \epsilon m_{2_r}) \in \hat{\mathcal{S}}^3$, and $\hat{m}_\omega := (m_{1_\omega} + \epsilon m_{2_v}) \in \hat{\mathbb{H}}^v$. In addition, let us define $r := (e_1, e_2, m_1, m_2) \in \mathbb{R}^{16}$. For simplicity, the robustness results are presented only for the hybrid system (10). Note that the result in this section also holds for the hybrid system with tracking model $\mathcal{H}_T$ in Eq. (38).

Following the fact that $\mathcal{H}$ is well-posed, and the global asymptotic stability property of set $\mathcal{A}$ for the closed-loop system $\mathcal{H}$ established in Theorem V.2 ([23], lemma 7.20) automatically leads to the following result about robustness of asymptotic stability:

*Theorem V.5:* Set $\mathcal{A}$ in Eq. (12) is semiglobally, practically robustly $\mathcal{KL}$ asymptotically stable for the closed-loop system $\mathcal{H}$; namely, there exists class-$\mathcal{KL}$ function $\beta$, such that, for each $\epsilon > 0$ and each compact set $\mathcal{M} \subset \mathcal{X}$, there exists $\rho > 0$, such that, for each measurable $r : \mathbb{R}_{\geq 0} \to \rho\mathbb{B}$, every solution $\phi$ to the hybrid system $\mathcal{H}$ with initial condition $\phi(0, 0) \in \mathcal{M}$ and perturbation $r$ satisfies

$$|\phi(t, j)|_{\mathcal{A}} \leq \beta(|\phi(0, 0)|_{\mathcal{A}}, t + j) + \epsilon \quad \forall\ (t, j) \in \text{dom}\phi \tag{40}$$

In Theorem V.5, "practical" means that the solutions to the hybrid system $\mathcal{H}$, in the presence of some small disturbances, converge $\epsilon > 0$ close to the desired set $\mathcal{A}$ in a semiglobal manner, namely, when the solutions start from arbitrary compact sets of initial conditions. A proof of this result is available in chapter 7 of [23].

## V. Simulations

### A. Simulation Parameters

To verify the ideas presented in this paper, we apply the hybrid hysteresis-based switching strategy to a rigid-body model with mass $m = 1$ kg and inertia

$$J = \begin{bmatrix} 1 & 0.1 & 0.15 \\ 0.1 & 0.63 & 0.05 \\ 0.15 & 0.05 & 0.85 \end{bmatrix} \text{kg} \cdot \text{m}^2$$

as in [36]. In the results presented as follows, each of the plots shows simulations of hybrid, discontinuous, and continuous controllers. For the simulations labeled hybrid, the hysteresis half-width $\delta \in (0, 1)$ and $h(t, j) \in \{-1, 1\}$. When the hysteresis width $\delta = 0$, the controller reduces to discontinuous scheme, where

$$h := \text{sgn}(\eta_r) = \begin{cases} -1 & \eta_r < 0 \\ 1 & \eta_r \geq 0 \end{cases} \tag{41}$$

When $\delta > 1$, $h = 1$ and a continuous controller exhibiting unwinding is implemented. To this end, simulations associated with full-state feedback using hybrid feedback (7–9), where the output of the system (6) is measured as $y = (\hat{q}_b, \hat{\omega}_b)$ [and hence, the error vector $(\overline{q}, \overline{\omega})$ is available for feedback], are presented in Sec. V.B. And the simulation results associated with the hybrid tracking feedback controller (35–37) with measurement of dual quaternion $\overline{q}_b$ are presented in Sec. IV.B. Following the results in Sec. IV.C, for all the simulation results as follows, the measured value of the pose $\overline{q}_m := \overline{q} + km_q/|\overline{q} + km_q|$, where $m_q = \boldsymbol{e}/|\boldsymbol{e}|$ is the normalized error. Each value of $\boldsymbol{e}$ is drawn from a zero-mean Gaussian distribution with unit variance; $k$ was drawn from a uniform distribution on the interval (0, 0.2) for set-point stabilization in Sec. V.B and the interval (0, 0.02) for the tracking control presented in Sec. V.C. This additional noise in the states results in chattering behavior for the switching signal $\text{sgn}(\eta_r)$ for the discontinuous controller, whereas the hysteresis-based hybrid logic is impervious to such noise, as shown

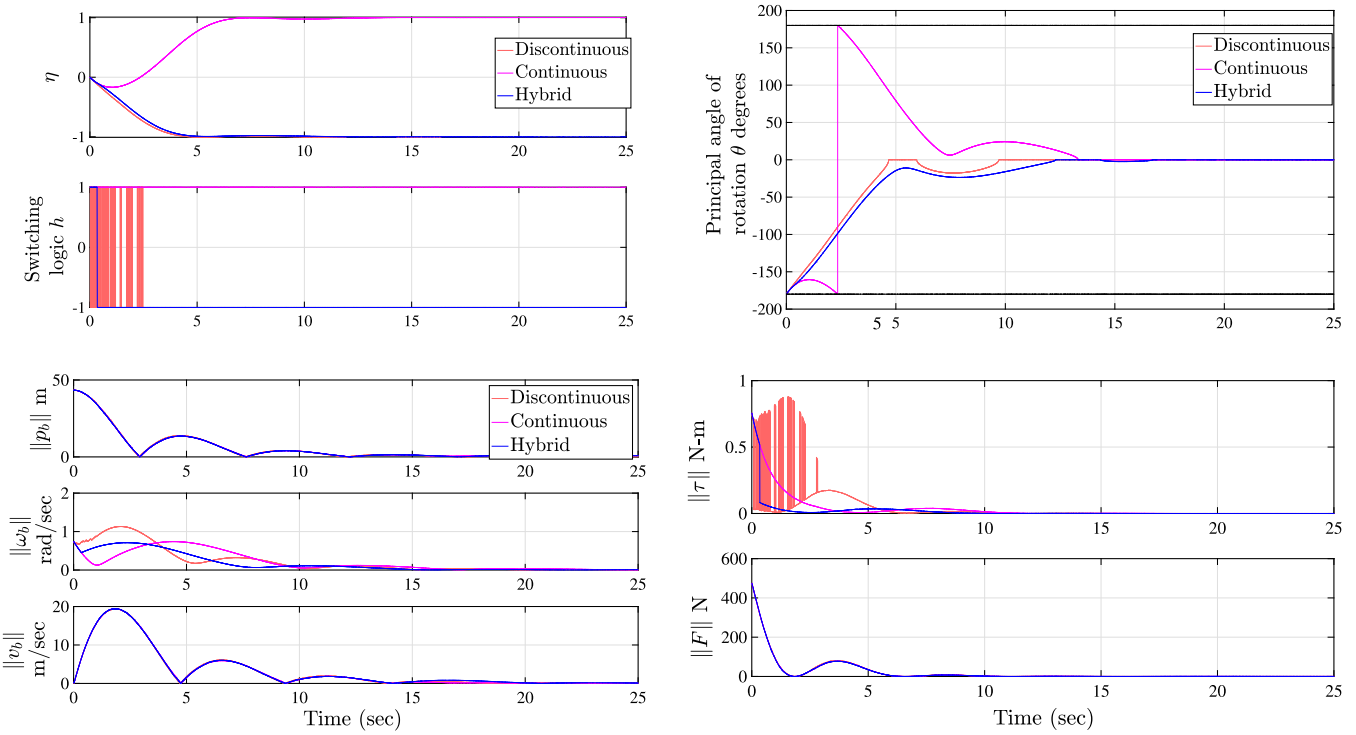


**Fig. 1 Closed-loop response of the controllers subjected to noise with the switching logic $h = 1$ and $\delta = 0.1$.**

in Figs. 1, 2, and 6 (code at https://github.com/HybridSystemsLab/DualQuaternionBasedHybridController).

### B. Set-Point Pose Stabilization

The response of the closed-loop rigid-body dynamics with hybrid feedback (7–9), when dual-quaternion error and velocity errors $(\overline{q}, \overline{\omega})$ are available for feedback, is presented in Fig. 1. The simulations are performed with the initial condition set to $p_b(0,0) = (25, 25, 25\ \text{m})$ (position in the body frame), velocity $v_b(0,0) = (0.1, 0.2, 0.3\ \text{m/s})$, and orientation $q_{b_r}(0,0) = (0, 0.4243, 0.5657, 0.7071)$, which corresponds to the principal angle of rotation, $\theta = 180$ deg, where $\theta := (\text{trace}(R) - 1)/2$, angular velocity $\omega_b(0,0) = (0.2, 0.4, 0.6\ \text{rad/s})$, and $h = 1$. The energy-based controller has the gains $k_d = 0.5$, $k_p = 0.5$ and a hysteresis gap of $\delta = 0.1$. Figure 1 also shows a comparison between the linear continuous controller with $h = 1$, a discontinuous controller where the switching logic variable $h := \text{sgn}(\eta_r)$ as in Eq. (41), and the hybrid controller with $h \in \{-1, 1\}$ as in Sec. IV.A. Next, we consider a larger hysteresis width of $\delta = 0.4$, and repeat the simulations with the same set of initial conditions and uncertainties as in the preceding analysis (Fig. 1). The hybrid controller now exhibits the same unwinding solution as the linear continuous controller due to the larger hysteresis gap. As discussed previously in [34], there is a correlation between hysteresis width $\delta$ and the sensitivity of the controller (7) to noise and the control effort, as shown in Figs. 1 and 2.

### C. Pose Tracking

To simulate the rigid-body pose tracking algorithm presented in Sec. IV.B, let us consider that the desired reference position and orientation satisfying Assumption V.3 are generated by the following dynamics:

$$\begin{aligned}
\dot{q}_d &= \frac{1}{2} q_d \otimes \nu(\omega^d_{d/I}) \\
\dot{q}_{d_t} &= \frac{1}{2} q_d \otimes \nu(v^d_{d/I}) + \frac{1}{2} q_{d_t} \otimes \nu(\omega^d_{d/I}) \\
\dot{\omega}^d_{d/I} &= 0_{3\times 1} \\
\dot{v}^d_{d/I} &= (0, 0, -0.0098) - \omega^d_{d/I} \times v^d_{d/I}
\end{aligned} \tag{42}$$

where $\omega^d_{d/I}$, $v^d_{d/I}$ are the angular and linear velocities of the desired frame with respect to the inertial frame expressed in the desired frame, respectively. With these sets of equations in Eq. (42), the reference pose to be tracked is generated using the following initial conditions: $q_d(0,0) = (1, 0, 0, 0)$, $q_{d_t}(0,0) = (0, 0, 0, 0)$, $\omega^d_{d/I} =$

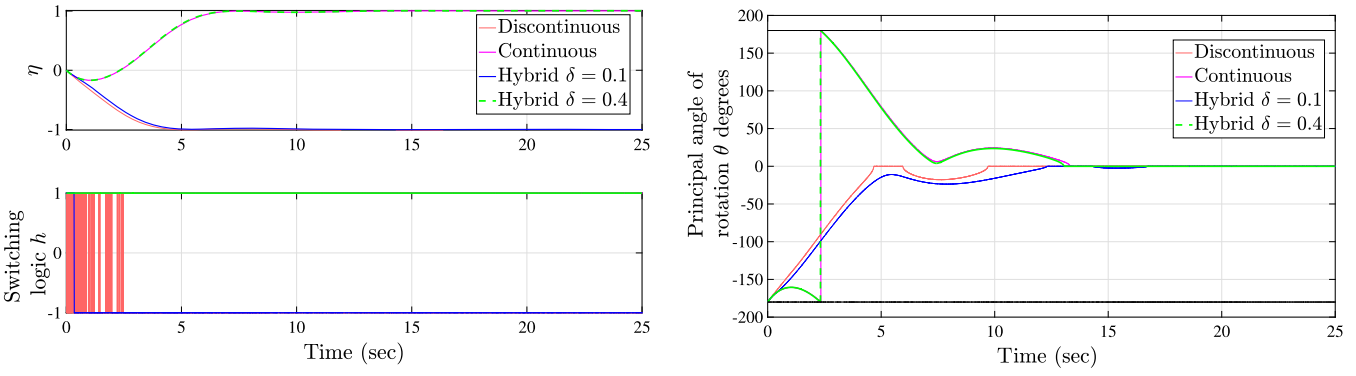


**Fig. 2 Unwinding in rigid-body rotational and translational dynamics with the switching logic $h = 1$ and $\delta = 0.4$.**

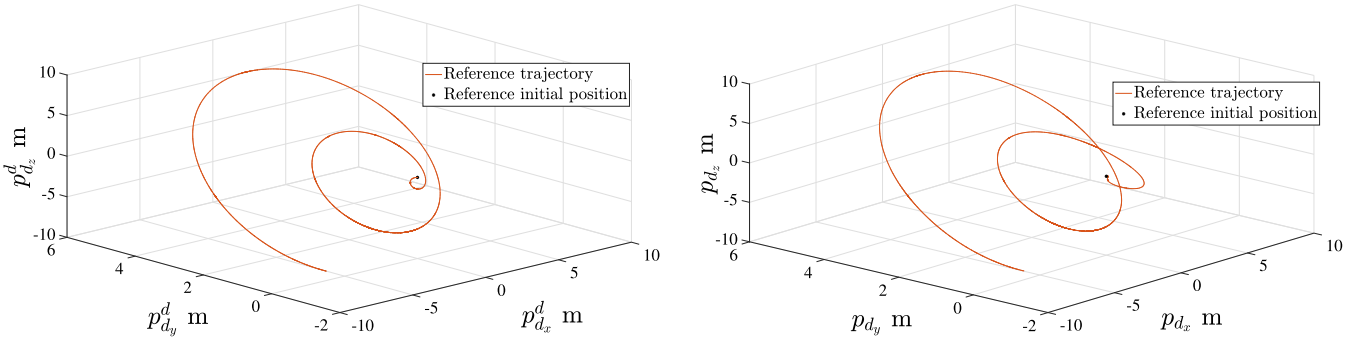


**Fig. 3 Reference trajectory generated with Eq. (42) and resolved into the desired, body frames of reference, respectively.**

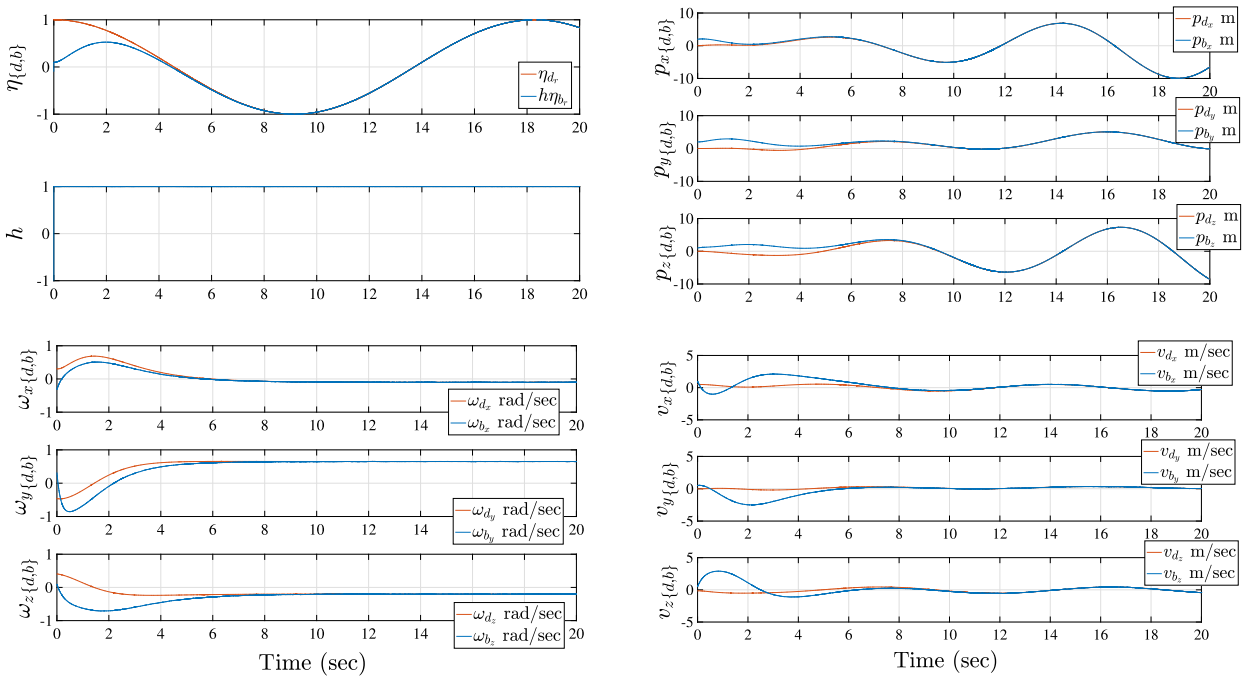


**Fig. 4 Rigid-body pose tracking with controller (35–37), $h = 1$, and $\delta = 0.4$ resolved into the rigid-body frame of reference.**

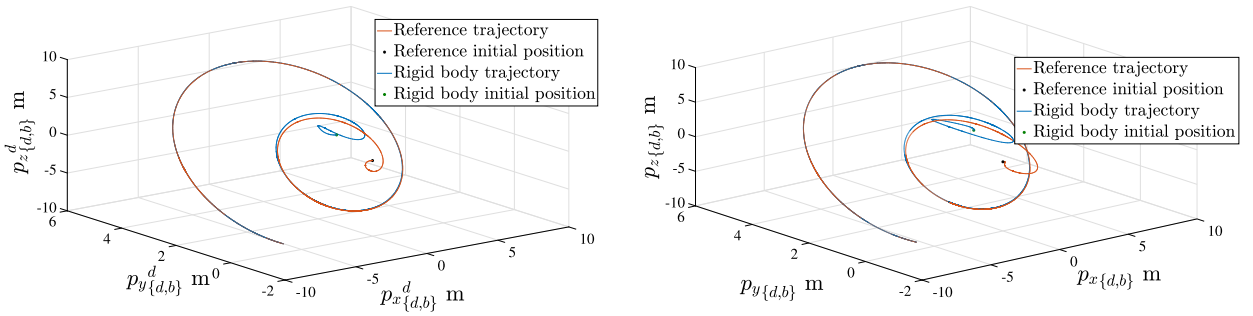


**Fig. 5 Desired and rigid-body trajectories expressed in desired frame of reference and rigid-body frame of reference, respectively.**

$(-0.1, 0.65, -0.2)$ rad/s, and $v^d_{d/I} = (-0.5, 0.1, 0.1)$ m/s. The corresponding reference trajectory is presented in Fig. 3. Next, the rigid body that tracks the reference pose in Fig. 3 has the dynamics as given in Eq. (2), and its initial conditions are given as follows: $q_{b_r}(0,0) = (0.1, 0.2659, 0.5318, 0.7978)$, $q_{b_t}(0,0) = (-1.1966, -0.4318, 0.7648, -0.2159)$, $p_b = (2, 2, 1)$ m (position in the body frame), $\omega_b = (-0.6, 0.6, 1)$ rad/s, and $v_b = (1, 0.5, 0.5)$ m/s. The hybrid feedback controller (35–37) is implemented with the gains $k_p = 4$, $k_d = 4$. Noise is added to the simulations, as discussed in Sec. V.A. As shown in Fig. 4, the rigid body tracks the reference orientation, position, and angular and linear velocities, respectively. In addition, Fig. 5 illustrates the position of the rigid body as seen in the rigid-body frame of reference and desired frame of reference.

As discussed in the set-point stabilization problem in Sec. V.B, a discontinuous controller where the switching logic variable $h := \text{sgn}(\eta_r)$ as in Eq. (41) would result in chattering and not tracking the desired reference, whereas a hybrid controller with $h \in \{-1, 1\}$ tracks the reference pose efficiently in the presence of measurement errors. These results are illustrated in Fig. 6.

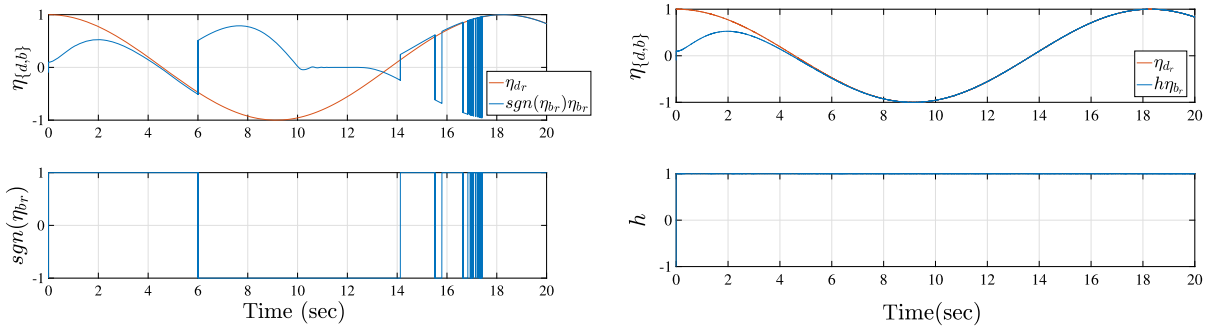


**Fig. 6 Rigid-body trajectories with discontinuous and hybrid controller, respectively.**

## VI. Conclusions

In this paper, a hybrid UDQ feedback control scheme was proposed for rigid-body robust pose stabilization with full state of the system available for feedback. The stability of the closed-loop system was guaranteed through an energy-based Lyapunov function analysis using invariance principles for hybrid systems presented as set-point stabilization and tracking problems. It has been shown that the proposed control schemes can globally asymptotically stabilize the kinematics and kinetics, and establish global asymptotic stability for a rigid-body. In addition, these proposed hybrid schemes allow for the controlled system to be stable in the presence of uncertainty, which would otherwise cause chattering about the point of discontinuous control. Simulation results for the rigid-body motion are presented. For future research directions, these results will be extended to the problem of spacecraft formation flying under orbit/attitude coupling forces and moments, such as atmospheric drag, gravity gradients, and solar radiation pressure, which make it impractical to design separate controllers for the translational and rotational dynamics.

## Appendix: Dual Quaternions

1) A set of quaternions (not necessarily normalized) are denoted by $\mathbb{H} := \{q: q = (\eta, \mu), \eta \in \mathbb{R}, \mu \in \mathbb{R}^3\}$, in which $\eta \in \mathbb{R}$ is the scalar part and $\mu \in \mathbb{R}^3$ is the vector part.

2) $\mathcal{S}^3$ denotes the set of unit quaternions, which is often used to parameterize the Lie group SO(3) of rigid-body attitude, where each unit quaternion is such that $|q|^2 = \eta^2 + \mu^\top \mu = 1$. Trivially, $\mathcal{S}^3 \subset \mathbb{H}$.

3) The set $\mathcal{S}^3$ has, under the quaternion product, an identity element $\mathbf{1} = (1, 0_{3\times1})$, and each $q = (\eta, \mu) \in \mathcal{S}^3$ has an inverse given by the quaternion conjugate $q^* = (\eta, -\mu)$.

Note that, given $q_1, q_2 \in \mathbb{H}$, where $q_1 = (\eta_1, \mu_1)$ and $q_2 = (\eta_2, \mu_2)$, under the quaternion multiplication rule, we have

$$q_1 \otimes q_2 = \begin{bmatrix} \eta_1\eta_2 - \mu_1^\top \mu_2 \\ \eta_1\mu_2 + \eta_2\mu_1 + \mu_1 \times \mu_2 \end{bmatrix}$$

4) The set of dual quaternions is given by

$$\hat{\mathbb{H}} := \{\hat{q}: \hat{q} = (\hat{\eta}, \hat{\mu}) = q_r + \epsilon q_t, q_r, q_t \in \mathbb{H}\}$$

where $\epsilon$ is the unit dual, defined as $\epsilon \neq 0$, $\epsilon^2 = 0$, and given $\hat{q} = (\hat{\eta}, \hat{\mu}) \in \hat{\mathbb{H}}$

a) $\hat{\eta} = \eta_r + \epsilon\eta_t$ is the dual scalar part, where $\eta_r, \eta_t \in \mathbb{R}$.
b) $\hat{\mu} = \mu_r + \epsilon\mu_t$ is the dual vector part, where $\mu_r, \mu_t \in \mathbb{R}^3$.
c) $q_r = (\eta_r, \mu_r) \in \mathbb{H}$, where $\eta_r \in \mathbb{R}$, $\mu_r \in \mathbb{R}^3$.
d) $q_t = (\eta_t, \mu_t) \in \mathbb{H}$, where $\eta_t \in \mathbb{R}$, $\mu_t \in \mathbb{R}^3$.

5) The space $\hat{\mathbb{H}}^v$ denotes the dual quaternions with zero scalar part [i.e., $\hat{\mathbb{H}}^v := \{\hat{q} = (\hat{\eta}, \hat{\mu}) \in \hat{\mathbb{H}}: \hat{\eta} = 0\}$].

6) The set of dual quaternions with zero vector part is given by $\hat{\mathbb{H}}^s := \{\hat{q} = (\hat{\eta}, \hat{\mu}) \in \hat{\mathbb{H}}: \hat{\mu} = 0_{3\times1}\}$.

7) Given a dual quaternion $\hat{q} \in \hat{\mathbb{H}}$, the following definitions hold:

a) Conjugate: $\hat{q}^* = q_r^* + \epsilon q_t^* = (\hat{\eta}, -\hat{\mu})$.
b) Swap: $\hat{q}^s = q_t + \epsilon q_r$

where $q^* = (\eta, -\mu)$ is the conjugate of a given quaternion $q = (\eta, \mu)$.

8) Given any dual quaternions $\hat{q}_1, \hat{q}_2, \hat{q}_3 \in \hat{\mathbb{H}}$, we define the following:

a) Dual-quaternion multiplication: $\hat{q}_1 \otimes \hat{q}_2 = q_{r_1} \otimes q_{r_2} + \epsilon(q_{r_1} \otimes q_{t_2} + q_{t_1} \otimes q_{r_2}) \in \hat{\mathbb{H}}$.
b) Dot product: $\hat{q}_1 \cdot \hat{q}_2 = (1/2)(\hat{q}_1^* \otimes \hat{q}_2 + \hat{q}_2^* \otimes \hat{q}_1) = (1/2)(\hat{q}_1 \otimes \hat{q}_2^* + \hat{q}_2 \otimes \hat{q}_1^*) = q_{r_1} \cdot q_{r_2} + \epsilon(q_{t_1} \cdot q_{r_2} + q_{r_1} \cdot q_{t_2}) \in \hat{\mathbb{H}}^s$.
c) Cross product: $\hat{q}_1 \times \hat{q}_2 = (1/2)(\hat{q}_1 \cdot \hat{q}_1 - \hat{q}_2^* \cdot \hat{q}_1^*) \in \hat{\mathbb{H}}^v$.
d) Circle product: $\hat{q}_1 \circ \hat{q}_2 = q_{r_1} \cdot q_{r_2} + q_{t_1} \cdot q_{t_2}$.
e) Dual norm: $\|\hat{q}\|^2 = \hat{q} \otimes \hat{q}^* = \hat{q}^* \otimes \hat{q} = \hat{q} \cdot \hat{q}$.
f) $M \star \hat{q} = (M_{11} q_r + M_{12} q_t) + \epsilon(M_{21} q_r + M_{22} q_t)$, $M_{ij} \in \mathbb{R}^{4\times4}$, $i, j \in \{1, 2\}$.

Note that, given a matrix $M \in \mathbb{R}^{4\times4}$ and a quaternion $q = (\eta, \mu) \in \mathbb{H}$

$$Mq = (m_{11}\eta + m_{12}\mu, m_{21}\eta + m_{22}\mu) \in \mathbb{H}$$

where $m_{11} \in \mathbb{R}$, $m_{12} \in \mathbb{R}^{1\times3}$, $m_{21} \in \mathbb{R}^{3\times1}$, and $m_{22} \in \mathbb{R}^{3\times3}$ are entries of

$$M = \begin{bmatrix} m_{11} & m_{12} \\ m_{21} & m_{22} \end{bmatrix}$$

9) The zero dual quaternion is given by $\hat{\mathbf{0}} = \mathbf{0} + \epsilon\mathbf{0}$.

10) The sub bullet points are the properties satisfied by the dual quaternions $\hat{q}_1, \hat{q}_2, \hat{q}_3 \in \hat{\mathbb{H}}$ satisfy the following properties:

a) $\hat{q}_1 \circ (\hat{q}_2 \otimes \hat{q}_3) = \hat{q}_2^s \circ (\hat{q}_1^s \otimes \hat{q}_3^*) = \hat{q}_3^s \circ (\hat{q}_2^* \otimes \hat{q}_1^s)$.
b) $\hat{q}_1 \circ (\hat{q}_2 \times \hat{q}_3) = \hat{q}_2^s \circ (\hat{q}_3 \times \hat{q}_1^s) = \hat{q}_3^s \circ (\hat{q}_1^s \times \hat{q}_2)$.
c) $(M \star \hat{q}_1) \circ \hat{q}_2 = \hat{q}_1 \circ (M^\top \star \hat{q}_2)$.
d) $\hat{q}_1 \circ \hat{q}_2 = \hat{q}_2 \circ \hat{q}_1$.
e) $\hat{q}_1^s \circ \hat{q}_2^s = \hat{q}_1 \circ \hat{q}_2$.
f) $(\hat{q}_1^s)^s = \hat{q}_1$.
g) $\hat{q}_1 \times \hat{q}_1 = \hat{\mathbf{0}}$.

11) The set of unit dual quaternions (UDQs) is denoted by $\hat{\mathcal{S}}^3$, where each UDQ $\hat{q} = q_r + \epsilon q_t \in \hat{\mathbb{H}}$, $q_r$, $q_t \in \mathbb{H}$, under the dual norm:

$$\|\hat{q}\|^2 = \hat{q} \otimes \hat{q}^* = \hat{q}^* \otimes \hat{q} = q_r \otimes q_r^* + \epsilon(q_r \otimes q_t^* + q_t \otimes q_r^*)$$

is such that $q_r \otimes q_r^* = \mathbf{1}$ and $q_r \otimes q_t^* + q_t \otimes q_r^* = \mathbf{0}$.

12) The set $\hat{\mathcal{S}}^3$ has, under the dual-quaternion multiplication, an identity element $\hat{\mathbf{1}}$, where $\hat{\mathbf{1}} = \mathbf{1} + \epsilon\mathbf{0}$, $\mathbf{1} = (1, 0_{3\times1})$, $\mathbf{0} = (0, 0_{3\times1})$, and the inverse given by the dual-quaternion conjugate $\hat{q}^*$.

13) Given an invertible matrix $M \in \mathbb{R}^{n\times n}$, we define the operation $M \star M^{-1} := I_n$.

## Acknowledgments

This material is based upon the work supported by the National Science Foundation under grant number CMMI-1561836. Research by R. G. Sanfelice has been partially supported by the National Science Foundation under grant numbers ECS-1710621 and CNS-1544396; the U.S. Air Force Office of Scientific Research under grant

numbers FA9550-16-1-0015, FA9550-19-1-0053, and FA9550-19-1-0169; and by CITRIS and the Banatao Institute at the University of California.

## References


[1] Sanyal, A., Fosbury, A., Chaturvedi, N., and Bernstein, D., "Inertia-Free Spacecraft Attitude Tracking with Disturbance Rejection and Almost Global Stabilization," *Journal of Guidance, Control, and Dynamics*, Vol. 32, No. 4, 2009, pp. 1167–1178. https://doi.org/10.2514/1.41565

[2] Chatuverdi, N. A., Sanyal, A. K., and McClamroch, N. H., "Rigid-Body Attitude Control Using Rotation Matrices for Continuous, Singularity-Free Control Laws," *IEEE Control Systems Magazine*, Vol. 31, No. 8, 2011, pp. 30–51.

[3] Joshi, S. M., Kelkar, A. G., and Wen, J.-Y., "Robust Attitude Stabilization of Spacecraft Using Nonlinear Quaternion Feedback," *IEEE Transactions on Automatic Control*, Vol. 40, No. 10, 1995, pp. 1800–1803. https://doi.org/10.1109/9.467669

[4] Li, S., Ding, S., and Li, Q., "Global Set Stabilization of the Spacecraft Attitude Control Problem Based on Quaternion," *International Journal of Robust and Nonlinear Control*, Vol. 20, No. 1, 2010, pp. 84–105. https://doi.org/10.1002/rnc.v20:1

[5] Kristiansen, R., Nicklasson, P., and Gravdahl, J., "Satellite Attitude Control by Quaternion-Based Backstepping," *IEEE Transactions on Control Systems Technology*, Vol. 17, No. 1, 2009, pp. 227–232. https://doi.org/10.1109/TCST.2008.924576

[6] Wisniewski, R., and Kulczycki, P., "Rotational Motion Control of a Spacecraft," *IEEE Transactions on Automatic Control*, Vol. 48, No. 4, 2003, pp. 643–646. https://doi.org/10.1109/TAC.2003.809781

[7] Schaub, H., and Junkins, J. L., *Analytical Mechanics of Space Systems*, AIAA, Reston, VA, 2003.

[8] Dooley, J. R., and McCarthy, J. M., "Spatial Rigid Body Dynamics Using Dual Quaternion Components," *Proceedings of the IEEE International Conference on Robotics and Automation*, Vol. 1, IEEE, New York, 1993, pp. 1031–1036.

[9] Murray, R. M., Li, Z., and Sastry, S. S., *A Mathematical Introduction to Robotic Manipulation*, CRC Press, Boca Raton, FL, 1994.

[10] Filipe, N., and Tsiotras, P., "Adaptive Position and Attitude-Tracking Controller for Satellite Proximity Operations Using Dual Quaternions," *Journal of Guidance, Control, and Dynamics*, Vol. 38, No. 4, 2015, pp. 566–577. https://doi.org/10.2514/1.G000054

[11] Wang, X., Yu, C., and Lin, Z., "A Dual Quaternion Solution to Attitude and Position Control for Rigid-Body Coordination," *IEEE Transactions on Robotics*, Vol. 28, No. 5, 2012, pp. 1162–1170. https://doi.org/10.1109/TRO.2012.2196310

[12] Nazari, M., Butcher, E. A., Yucelen, T., and Sanyal, A. K., "Decentralized Consensus Control of a Rigid-Body Spacecraft Formation with Communication Delay," *Journal of Guidance, Control, and Dynamics*, Vol. 39, No. 4, 2016, pp. 838–851. https://doi.org/10.2514/1.G001396

[13] Li, X., Zhu, Z., and Song, S., "Non-Cooperative Autonomous Rendezvous and Docking Using Artificial Potentials and Sliding Mode Control," *Proceedings of the Institution of Mechanical Engineers, Part G: Journal of Aerospace Engineering*, Vol. 233, No. 4, 2019, pp. 1171–1184. https://doi.org/10.1177/0954410017748988

[14] Sanyal, A., Holguin, L., and Viswanathan, S., "Guidance and Control for Spacecraft Autonomous Chasing and Close Proximity Maneuvers," *IFAC Proceedings Volumes*, Vol. 45, No. 13, 2012, pp. 753–758. https://doi.org/10.3182/20120620-3-DK-2025.00068

[15] Sarlette, A., Bonnabel, S., and Sepulchre, R., "Coordinated Motion Design on Lie Groups," *IEEE Transactions on Automatic Control*, Vol. 55, No. 5, 2010, pp. 1047–1058. https://doi.org/10.1109/TAC.2010.2042003

[16] Bullo, F., and Murray, R. M., "Tracking for Fully Actuated Mechanical Systems: A Geometric Framework," *Automatica*, Vol. 35, No. 1, 1999, pp. 17–34. https://doi.org/10.1016/S0005-1098(98)00119-8

[17] Cunha, R., Silvestre, C., and Hespanha, J., "Output-Feedback Control for Stabilization on $SE(3)$," *Systems & Control Letters*, Vol. 57, No. 12, 2008, pp. 1013–1022. https://doi.org/10.1016/j.sysconle.2008.06.008

[18] Bhat, S. P., and Bernstein, D. S., "A Topological Obstruction to Continuous Global Stabilization of Rotational Motion and the Unwinding Phenomenon," *Systems & Control Letters*, Vol. 39, No. 1, 2000, pp. 63–70. https://doi.org/10.1016/S0167-6911(99)00090-0

[19] Sanyal, A. K., and Chaturvedi, N. A., "Almost Global Robust Attitude Tracking Control of Spacecraft in Gravity," *AIAA Guidance, Navigation, and Control Conference and Exhibit*, AIAA Paper 2008-6979, Aug. 2008.

[20] Fjellstad, O., and Fossen, T. I., "Quaternion Feedback Regulation of Underwater Vehicles," *Proceedings of IEEE International Conference on Control and Applications*, Vol. 2, IEEE, New York, 1994, pp. 857–862.

[21] Fragopoulos, D., and Innocenti, M., "Stability Considerations in Quaternion Attitude Control Using Discontinuous Lyapunov Functions," *IEE Proceedings—Control Theory and Applications*, Vol. 151, No. 3, 2004, pp. 253–258. https://doi.org/10.1049/ip-cta:20040311

[22] Mayhew, C. G., and Teel, A. R., "On the Topological Structure of Attraction Basins for Differential Inclusions," *Systems & Control Letters*, Vol. 60, No. 12, 2011, pp. 1045–1050. https://doi.org/10.1016/j.sysconle.2011.07.012

[23] Goebel, R., Sanfelice, R. G., and Teel, A. R., *Hybrid Dynamical Systems: Modeling, Stability, and Robustness*, Princeton Univ. Press, Princeton, NJ, 2012.

[24] Mayhew, C. G., Sanfelice, R. G., and Teel, A. R., "On Path-Lifting Mechanisms and Unwinding in Quaternion-Based Attitude Control," *IEEE Transactions on Automatic Control*, Vol. 58, No. 5, 2013, pp. 1179–1191, http://ieeexplore.ieee.org/xpls/abs_all.jsp?arnumber=6389715.

[25] Mayhew, C. G., and Teel, A. R., "Synergistic Potential Functions for Hybrid Control of Rigid-Body Attitude," *Proceedings of the 2011 American Control Conference*, IEEE, New York, 2011, pp. 875–880.

[26] Berkane, S., and Tayebi, A., "Construction of Synergistic Potential Functions on SO(3) with Application to Velocity-Free Hybrid Attitude Stabilization," *IEEE Transactions on Automatic Control*, Vol. 62, No. 1, 2017, pp. 495–501. https://doi.org/10.1109/TAC.2016.2560537

[27] Berkane, S., Abdessameud, A., and Tayebi, A., "Global Hybrid Attitude Estimation on the Special Orthogonal Group SO(3)," *American Control Conference (ACC), 2016*, IEEE, New York, 2016, pp. 113–118.

[28] Berkane, S., Abdessameud, A., and Tayebi, A., "On the Design of Globally Exponentially Stable Hybrid Attitude and Gyro-Bias Observers," arXiv preprint arXiv:1605.05640, 2016.

[29] Casau, P., Sanfelice, R. G., Cunha, R., Cabecinhas, D., and Silvestre, C., "Robust Global Trajectory Tracking for a Class of Underactuated Vehicles," *Automatica*, Vol. 58, Aug. 2015, pp. 90–98. https://doi.org/10.1016/j.automatica.2015.05.011

[30] Casau, P., Sanfelice, R. G., Cunha, R., and Silvestre, C., "A Globally Asymptotically Stabilizing Trajectory Tracking Controller for Rigid Bodies Using Only Landmark-Based Information," *International Journal of Robust and Nonlinear Control*, Vol. 25, No. 18, 2015, pp. 3617–3640. https://doi.org/10.1002/rnc.3283

[31] Clifford, W. K., "Preliminary Sketch of Bi-Quaternions," *Proceedings of London Mathematical Society*, Vols. 1–4, No. 1, Nov. 1873, pp. 381–395.

[32] Study, E., *Geometrie der Dynamen: Die Zusammensetzung von kräften und verwandte Gegenstände der Geometrie*, B.G. Teubner, Leipzig, Germany, 1901.

[33] Sanfelice, R. G., Messina, M. J., Tuna, S. E., and Teel, A. R., "Robust Hybrid Controllers for Continuous-Time Systems with Applications to Obstacle Avoidance and Regulation to Disconnected Set of Points," *Proceedings of the 25th American Control Conference*, IEEE, New York, 2006, pp. 3352–3357, http://ieeexplore.ieee.org/iel5/11005/34689/01657236.pdf?tp=&isnumber=&arnumber=1657236, https://hybrid.soe.ucsc.edu/files/preprints/7.pdf.

[34] Mayhew, C. G., Sanfelice, R. G., and Teel, A. R., "Quaternion-Based Hybrid Controller for Robust Global Attitude Tracking," *IEEE Transactions on Automatic Control*, Vol. 56, No. 11, 2011, pp. 2555–2566, http://ieeexplore.ieee.org/xpl/freeabs_all.jsp?arnumber=5701762, https://hybrid.soe.ucsc.edu/files/preprints/50.pdf. https://doi.org/10.1109/TAC.2011.2108490

[35] Kussaba, H. M., Figueredo, L. F. C., Ishihara, J., and Adorno, B. V., "Hybrid Kinematic Control for Rigid Body Pose Stabilization Using Dual Quaternions," *Journal of the Franklin Institute*, Vol. 354, No. 7, 2017, pp. 2769–2787. https://doi.org/10.1016/j.jfranklin.2017.01.028

[36] Filipe, N., and Tsiotras, P., "Simultaneous Position and Attitude Control Without Linear and Angular Velocity Feedback Using Dual

Quaternions," *Proceedings of the IEEE American Control Conference*, IEEE, New York, 2013, pp. 4808–4813.

[37] Filipe, N., and Tsiotras, P., "Rigid Body Motion Tracking Without Linear and Angular Velocity Feedback Using Dual Quaternions," *2013 European Control Conference (ECC)*, IEEE, New York, 2013, pp. 329–334.

[38] Han, D.-P., Wei, Q., and Li, Z.-X., "Kinematic Control of Free Rigid Bodies Using Dual Quaternions," *International Journal of Automation and Computing*, Vol. 5, No. 3, 2008, pp. 319–324. https://doi.org/10.1007/s11633-008-0319-1

[39] Wang, X., and Yu, C., "Unit Dual Quaternion-Based Feedback Linearization Tracking Problem for Attitude and Position Dynamics," *Systems & Control Letters*, Vol. 62, No. 3, 2013, pp. 225–233. https://doi.org/10.1016/j.sysconle.2012.11.019

[40] Magro, P. P. M., Kussaba, H. M., Figueredo, L. F. C., and Ishihara, J., "Dual Quaternion-Based Bimodal Global Control for Robust Rigid Body Pose Kinematic Stabilization," *Proceedings of the American Control Conference*, IEEE, New York, 2017, pp. 1205–1210.

[41] Lee, U., and Mesbahi, M., "Constrained Autonomous Precision Landing via Dual Quaternions and Model Predictive Control," *Journal of Guidance, Control, and Dynamics*, Vol. 40, No. 2, 2017, pp. 292–308. https://doi.org/10.2514/1.G001879

[42] Dong, H., Hu, Q., and Akella, M. R., "Dual-Quaternion-Based Spacecraft Autonomous Rendezvous and Docking Under Six-Degree-of-Freedom Motion Constraints," *Journal of Guidance, Control, and Dynamics*, Vol. 41, No. 5, 2018, pp. 1150–1162. https://doi.org/10.2514/1.G003094

[43] Wu, Y., Hu, X., Hu, D., Li, T., and Lian, J., "Strapdown Inertial Navigation System Algorithms Based on Dual Quaternions," *IEEE Transactions on Aerospace and Electronic Systems*, Vol. 41, No. 1, 2005, pp. 110–132. https://doi.org/10.1109/TAES.2005.1413751

[44] Wang, J., and Sun, Z., "6-DOF Robust Adaptive Terminal Sliding Mode Control for Spacecraft Formation Flying," *Acta Astronautica*, Vol. 73, April 2012, pp. 76–87. https://doi.org/10.1016/j.actaastro.2011.12.005